THE JOURNAL OF BIOLOGICAL CHEMISTRY VOL. 281, NO. 16, pp. 11058–11065, April 21, 2006

Interactions of GTP with the ATP-grasp Domain of GTP-specific Succinyl-CoA Synthetase*

Received for publication, November 1, 2005, and in revised form, February 2, 2006 Published, JBC Papers in Press, February 15, 2006, DOI 10.1074/jbc.M511785200

Marie E. Fraser[‡1], **Koto Hayakawa**[‡], **Millicent S. Hume**[§2], **David G. Ryan**[¶3], **and Edward R. Brownie**[‡]

From the [‡]*Department of Biological Sciences, University of Calgary, Calgary, Alberta T2N 1N4, the* [§]*Department of Biochemistry, The University of Western Ontario, London, Ontario N6A 5C1, and the* [¶]*Department of Biochemistry, University of Alberta, Edmonton, Alberta T6G 2H1, Canada*

Two isoforms of succinyl-CoA synthetase exist in mammals, one specific for ATP and the other for GTP. The GTP-specific form of pig succinyl-CoA synthetase has been crystallized in the presence of GTP and the structure determined to 2.1 Å resolution. GTP is bound in the ATP-grasp domain, where interactions of the guanine base with a glutamine residue (Gln-20*β*) and with backbone atoms provide the specificity. The *γ*-phosphate interacts with the side chain of an arginine residue (Arg-54*β*) and with backbone amide nitrogen atoms, leading to tight interactions between the *γ*-phosphate and the protein. This contrasts with the structures of ATP bound to other members of the family of ATP-grasp proteins where the *γ*-phosphate is exposed, free to react with the other substrate. To test if GDP would interact with GTP-specific succinyl-CoA synthetase in the same way that ADP interacts with other members of the family of ATP-grasp proteins, the structure of GDP bound to GTP-specific succinyl-CoA synthetase was also determined. A comparison of the conformations of GTP and GDP shows that the bases adopt the same position but that changes in conformation of the ribose moieties and the *α*- and *β*-phosphates allow the *γ*-phosphate to interact with the arginine residue and amide nitrogen atoms in GTP, while the *β*-phosphate interacts with these residues in GDP. The complex of GTP with succinyl-CoA synthetase shows that the enzyme is able to protect GTP from hydrolysis when the active-site histidine residue is not in position to be phosphorylated.

The enzyme succinyl-CoA synthetase (SCS)[4] uses ATP or GTP to catalyze the formation of succinyl-CoA from succinate and coenzyme A. In animals, two different isoforms exist, one specific for ATP and the other specific for GTP (1). The two isoforms include the same *α*-subunit, but different *β*-subunits (2). The amino-terminal domain of the *β*-subunit has an ATP-grasp fold (3–5), and Mg^{2+}-ADP was shown to bind in this domain of the *Escherichia coli* SCS using labeling experiments and site-directed mutagenesis (6) and by soaking the nucleotide into crystals and determining the structure of the resulting complex (7). The ATP-grasp fold has been found in a number of other enzymes (8), *e.g.* glutathione synthetase (9, 10), D-Ala:D-Ala ligase (11), D-Ala:D-lactate ligase (12, 13), LysX (14), biotin carboxylase (15), glycinamide ribonucleotide synthetase (16), N^5-carboxyaminoimidazole ribonucleotide synthetase (17), glycinamide ribonucleotide transformylase (18), carbamoyl phosphate synthetase (19), synapsin (20), pyruvate phosphate dikinase (10, 21), DNA ligases (22, 23), an mRNA capping enzyme (24), and RNA ligase 2 (25). The determinations of the structures of several of these enzymes in complex with nucleotides, nucleotide analogues, and their other substrates has led to a good understanding of the interactions that are important in their binding and catalysis.

The biological roles of the ATP- and GTP-specific SCS have not been fully delineated. Originally it was thought that the primary role for SCS was in the citric acid cycle, where it was responsible for the breakdown of succinyl-CoA to succinate and coenzyme A accompanied by the phosphorylation of nucleotide diphosphate to nucleotide triphosphate (26). This step provides the only substrate-level phosphorylation of the citric acid cycle. It was thought that some species had SCS that could use either ADP or GDP, *e.g. E. coli* (27), while others had SCS that could use only GDP, *e.g.* animals (26) or ADP, *e.g.* plants (28). Since the currency for energy in the cell is ATP, the GTP produced in the citric acid cycle would have to be converted to ATP by nucleotide diphosphate kinase. Once it was discovered that some animals had two forms of SCS, one specific for each nucleotide, it was hypothesized that the two isoforms allowed SCS to serve different metabolic roles (29). The reaction catalyzed by SCS is reversible and the direction would depend on the relative concentrations of nucleotide diphosphate and nucleotide triphosphate (30). Mammalian SCS is found in mitochondria where the ratio of the concentration of ATP to that of ADP is ~1, while the ratio of the concentration of GTP to that of GDP is ~100 (31). The high concentration ratio of GTP to GDP would drive the reaction in the opposite direction to that in the citric acid cycle (32), thus GTP-specific SCS might serve in the synthesis of succinyl-CoA, while ATP-specific SCS would serve in the citric acid cycle. In addition to breaking down succinyl-CoA, SCS catalyzes the reverse reaction to produce succinyl-CoA, an essential precursor in the synthesis of heme (33). Recent experiments have shown that both enzymes are produced in many tissues but the relative amounts vary (34). Tissues with high need for energy, such as the heart, do show higher activities of ATP-specific SCS, while kidney and liver tissues show higher activities of GTP-specific SCS. These relative activities are consistent with ATP-specific SCS serving a catabolic role, while GTP-specific SCS would serve an anabolic role. That said, the recent discovery of a deficiency of ATP-specific SCS activity associated with encephalomyopathy and mitochondrial DNA depletion (35) does suggest that ATP-specific SCS also serves an anabolic role.

* This work was supported by a Discovery Grant from the Natural Sciences and Engineering Research Council of Canada (NSERC) and made use of equipment funded by NSERC and by an Establishment Grant from Alberta Heritage Foundation for Medical Research. The costs of publication of this article were defrayed in part by the payment of page charges. This article must therefore be hereby marked "*advertisement*" in accordance with 18 U.S.C. Section 1734 solely to indicate this fact.

The atomic coordinates and structure factors (codes 2FPI (nucleotide-free), 2FPP (nucleotide-free with chloride ions), 2FP4 (complex with GTP), and 2FPG (complex with GDP)) have been deposited in the Protein Data Bank, Research Collaboratory for Structural Bioinformatics, Rutgers University, New Brunswick, NJ (http://www.rcsb.org/).

[1] A Biomedical Scholar supported by Alberta Heritage Foundation for Medical Research. To whom correspondence should be addressed: Dept. of Biological Sciences, University of Calgary, 2500 University Dr. NW, Calgary, Alberta T2N 1N4, Canada. Tel.: 403-220-6145; Fax: 403-289-9311; E-mail: frasm@ucalgary.ca.

[2] Present address: Amgen Canada Inc., 6755 Mississauga Rd., Suite 400, Mississauga, Ontario L5N 7Y2, Canada.

[3] Present address: Dept. of Dermatology, Feinberg School of Medicine, 303 East Chicago Ave., Ward Bldg. 9-124, Chicago, IL 60611.

[4] The abbreviations used are: SCS, succinyl-CoA synthetase; PMSF, phenylmethylsulfonyl fluoride; Bicine, *N*,*N*-bis(2-hydroxyethyl)glycine.

The structure of pig GTP-specific SCS has been determined in both the phosphorylated and dephosphorylated forms (36). In the catalytic reaction, His-259 of the α-subunit (designated His-259α) is transiently phosphorylated. Based on work with *E. coli* SCS, it was hypothesized that this active site histidine residue serves to shuttle the phosphoryl group between the nucleotide-binding site and the site where CoA and, presumably, succinate bind (5).

In this work, pig GTP-specific SCS has been crystallized in a complex with GTP to determine which residues provide nucleotide specificity. The structures of pig GTP-specific SCS without nucleotide and with GDP, crystallized under similar conditions to the GTP complex, have also been determined and are described here. These structures and the structures of other members of the ATP-grasp family provide useful comparisons for interpreting the binding of GTP to succinyl-CoA synthetase.

EXPERIMENTAL PROCEDURES

Protein Expression—The two subunits of pig GTP-specific SCS were cloned and overexpressed in *E. coli*. The amino termini of both subunits were modified by PCR to remove the signal sequences that target the polypeptides to mitochondria. The modifications of the α-subunit result in translation beginning at the NH_2-terminal sequence MSYTA, and post-translational modification removes the first methionine residue. The β-subunit begins with the amino acids MNLQ and the amino-terminal methionine residue is not cleaved. The design of the gene is different from one used earlier (37) because the crystal structure showed that a methionine residue inserted before the first residue of the mature β-subunit could interfere with catalysis (36). It may be the reason for the reduced specific activity of the enzyme produced in *E. coli* (37). Modified cDNAs encoding the mature α- and β-subunits were cloned into a single expression plasmid, each cDNA being placed downstream of a separate T7 promoter. *E. coli* BL21(DE3) were transformed with the plasmid. For protein expression, 500 ml of Luria-Bertani medium was inoculated and grown overnight at 30 °C. The cells were then diluted by a factor of twenty and allowed to grow until they reached an $A_{600\ nm}$ of 0.4. Protein expression was induced with 1.0 mM isopropyl β-D-thiogalactopyranoside and the cells were grown overnight at 30 °C. The cells were harvested by centrifugation in a Sorvall GSA rotor at 5×10^3 rpm and 4 °C for 30 min and then resuspended in 0.1 M KCl, 50 mM potassium phosphate, 1.0 mM benzamidine, 0.1 mM phenylmethylsulfonyl fluoride (PMSF), 0.1 mM EDTA, and 10 mM 2-mercaptoethanol, pH 7.4. After freezing at −70 °C, the cells were thawed and sonicated. The debris was pelleted by centrifugation at 1×10^4 rpm in a Sorvall SS34 rotor at 4 °C, and the supernatant was retained. The pellet was then resuspended, resonicated, and recentrifuged, again retaining the supernatant.

Protein Purification—Pig GTP-specific SCS was purified by ammonium sulfate fractionation and column chromatography at 4 °C. 20 g of ammonium sulfate were added to each 100 ml of supernatant, and after centrifugation at 1×10^4 rpm in the SS34 rotor, the precipitate was discarded. 30 g of ammonium sulfate were added per 100 ml of the original volume, and the sample was centrifuged. The supernatant was discarded, and the precipitate was redissolved in 10 mM potassium phosphate, 0.1 mM EDTA, 0.1 mM PMSF, 10.0 mM 2-mercaptoethanol, and 1.0 mM benzamidine, pH 7.4. The solution was loaded onto a 5.0 × 19-cm G-Sephadex Coarse column and eluted with 10 mM potassium phosphate, 0.1 mM EDTA, 0.1 mM PMSF, 10 mM 2-mercaptoethanol, and 1.0 mM benzamidine for desalting. To separate pig GTP-specific SCS from *E. coli* SCS, the protein was loaded on a hydroxyapatite column (5.0 × 10 cm) and eluted using a gradient of the buffer in which the concentration of potassium phosphate increased to 0.5 M. The protein was again precipitated with ammonium sulfate and redissolved in a minimal volume of buffer, then run on a Q-Sepharose Fast Flow column (5.0 × 10 cm). The column was washed with 10 mM potassium phosphate, 0.1 mM EDTA, pH 7.4, and eluted using a gradient increasing the potassium chloride concentration to 0.5 M. The protein was precipitated in 50% w/v ammonium sulfate, 10 mM potassium phosphate, 10 mM 2-mercaptoethanol, 0.2 mM PMSF, 0.2 mM EDTA, 1.0 mM benzamidine, pH 7.4, and stored at 4 °C. The final yield was ~13 mg of enzyme per liter of initial culture when using a fermentor and half that when using 2.8-liter Fernbach flasks.

The concentration and activity of pig GTP-specific SCS were measured spectrophotometrically. The concentration was determined from the absorbance at a wavelength of 280 nm using the absorption coefficient 0.35 A mg^{-1} cm^{-1} (38). The activity of the enzyme was measured in 0.11 M Tris-HCl, 0.05 M sodium succinate, 0.01 M $MgCl_2$, 0.1 M KCl, 0.1 mM GTP, 0.1 mM CoA, 0.1 mM diethyldithiothreitol by following the increase in absorption at 235 nm (39). Purified protein had a specific activity of 21 units mg^{-1}, twice the activity provided by the previous clone (37).

Crystallization—For crystallization, an aliquot of the ammonium sulfate precipitate was collected by centrifugation for 60 min at 12×10^3 rpm in the SS34 rotor. The precipitate was resuspended in a minimal volume of 50 mM potassium phosphate, pH 7.4. The protein solution was then dialyzed against 50 mM potassium phosphate, pH 7.4, and 1 mM 2-mercaptoethanol to remove ammonium sulfate. The dialysis bag was then transferred to a solution of 50 mM Bicine, pH 7.6, 0.5 mM GTP, 5 mM $MgCl_2$, 1 mM 2-mercaptoethanol overnight to phosphorylate His-259α. Dialysis in fresh phosphate buffer followed for a period of 24 h to remove the nucleotide, followed by dialysis in 50 mM HEPES, pH 7.4, or 50 mM Bicine, pH 7.6. The protein solution was removed from the dialysis tubing and centrifuged for 30 min at 30×10^3 rpm in a Beckman TLA 100 rotor at 4 °C to remove particulate matter.

Crystals were grown by vapor diffusion in hanging drops. The concentration of the protein was ~8 mg/ml, and a 1–2-μl drop of this solution was mixed with an equal volume of the precipitant solution, then hung over a 1-ml well of the precipitant solution. The first diffracting crystals were obtained using a precipitant solution containing 10% v/v isopropanol, 100 mM ammonium sulfate, 20% w/v polyethylene glycol 4000, and 100 mM HEPES or Bicine, pH 7.5. Crystals were visible within 2 or 3 days. The crystals diffracted better when the pH of the buffer was adjusted with hydrochloric acid, later realized to be due to the chloride ions. In initial unsuccessful attempts to obtain crystals with nucleotide bound, crystals were soaked in mother liquor containing 10 mM GDP and 25 mM $MgCl_2$. Crystals of the complex with GTP were successfully grown from a protein solution containing 5 mM GTP and 10 mM $MgCl_2$ using 20% w/v polyethylene glycol 3350 and 150 mM KF in the precipitant solution. Crystals of the complex with GDP were grown by seeding small crystals of the GTP complex into drops set up using 5 mM GDP instead of GTP. The seeds that formed were transferred into fresh drops and allowed to grow.

Data Collection and Structure Determination—Diffraction data were collected in house and at two synchrotrons. The in-house system was a Mar345 image plate detector on a rotating anode (Rigaku RU H3R, CuKα, 46 kV, 100 mA) with Osmic multilayer mirrors. Synchrotron data were collected at beamline 14-BM-C of the Advanced Photon Source and at beamline 8.3.1 of the Advanced Light Source using an ADSC CCD detector. For data collections at low temperature, the crystals were cryoprotected using mother liquor containing 10% v/v 2-methyl-2,4-pentanediol instead of isopropanol and 15% v/v glycerol

TABLE 1
Statistics for the data sets and refined models

Structure	Nucleotide-free	Nucleotide-free with Cl^-	Complex with GTP	Complex with GDP
X-ray source	Advanced Photon Source	In-house	Advanced Light Source	Advanced Light Source
Resolution range (high resolution)	35–2.7 Å (2.75–2.7 Å)	25–2.35 (2.43–2.35 Å)	73–2.1 Å (2.21–2.1 Å)	116–2.96 Å (3.12–2.96 Å)
R_{merge} (high resolution)[a]	4.9% (25.8%)	11.4% (37.4%)	5.5% (36.2%)	12.6% (53.2%)
$\langle I\rangle/\sigma(\langle I\rangle)$ (high resolution)[b]	35.4 (6.1)	13.1 (3.8)	19.8 (3.3)	10.9 (3.0)
Number of observations	134,763	120,730	238,302	98,686
Average redundancy	5.9	4.5	5.5	6.3
Completeness	99.8% (100%)	87.9% (77.3%)	99.6% (97.5%)	100% (100%)
Cell dimensions	$a = b = 135.8$ Å, $c = 77.2$ Å, $\alpha = \beta = 90°$, $\gamma = 120°$	$a = b = 123.4$ Å, $c = 84.9$ Å, $\alpha = \beta = 90°$, $\gamma = 120°$	$a = b = 132.6$ Å, $c = 72.5$ Å, $\alpha = \beta = 90°$, $\gamma = 120°$	$a = b = 133.8$ Å, $c = 73.1$ Å, $\alpha = \beta = 90°$, $\gamma = 120°$
Number of data for refinement	22,397	26,978	43,846	15,696
***R*-factor (number of data)**[c]	21.5% (21,274)	19.2% (25,907)	19.5% (41,251)	20.1% (14,892)
***R*-free (number of data)**[d]	31.0% (1123)	25.9% (1071)	24.2% (2235)	27.5% (804)
Number of protein atoms	5225	5225	5225	5221
Number of water molecules	64	126	294	10
Number of atoms in ions or ligands	10	16	66	34
Root mean square deviations from ideal geometry:				
Bond lengths (Å)	0.016	0.017	0.016	0.008
Bond angles (°)	2.0	1.9	1.9	1.4
Ramachandran plot:				
Number in most favored regions	503 (85.7%)	530 (90.3%)	543 (92.5%)	485 (82.6%)
Number in additional allowed regions	80 (13.6%)	57 (9.7%)	44 (7.5%)	101 (17.2%)
Number in generously allowed regions	4 (0.7%)	0	0	1 (0.2%)

[a] $R_{merge} = (\sum\sum|I_i - \langle I\rangle|)/\sum\sum\langle I\rangle$, where I_i is the intensity of an individual measurement of a reflection, and $\langle I\rangle$ is the mean value for all equivalent measurements of this reflection.
[b] $\langle I\rangle$ is the mean intensity for all reflections, $\langle\sigma(I)\rangle$ is the mean sigma for these reflections.
[c] *R*-factor $= \sum||F_o| - |F_c||/\sum|F_o|$.
[d] *R*-factor based on data excluded from the refinement (~5%).

for the crystals without nucleotide and 5% v/v glycerol for crystals with nucleotide. The crystals were vitrified at 100 K in the cold stream of gaseous nitrogen (Oxford Cryostream). Diffraction data were processed using the programs Denzo and Scalepack (40) or the Elves scripts (41) and programs from the CCP4 package (42).

The structures were solved by molecular replacement using the model of pig GTP-specific SCS identified in the Protein Data Bank (43) as 1EUD (36) and the program AMoRe (44) or by difference Fourier techniques. There is one molecule per asymmetric unit. The Crystallography and NMR System (45) was used for refinement. The programs TOM (ALBERTA/CALTECH version 3.0) (46) and XFIT (47) were used to visualize the maps and models and adjust the models. Model quality was judged using the programs PROCHECK (48) and WHATCHECK (49). Programs from the CCP4 package (42) as well as SwissPdbViewer (50), O (51), and DynDom (52) were used to analyze the models.

RESULTS

Four structures were determined: two with no nucleotide bound, plus the complex with GTP and the complex with GDP. The statistics for the four data sets and refined models are presented in Table 1. Each data set was collected from a single crystal, except for the data set for nucleotide-free GTP-specific SCS with the chloride ion. In this case, data were merged from two crystals, one of which diffracted to higher resolution than the other. (An equipment failure during the collection of the diffraction data from the better diffracting crystal led to the loss of that crystal.) The two structures with no nucleotide bound diffracted to different resolutions. The better diffracting crystals were grown with chloride, and electron density that was interpreted as the chloride ion was visible at a crystal-packing interface. Unfortunately, the chloride ion trapped the ATP-grasp domain in a more open conformation, likely leading to the lack of success in binding nucleotide to the protein in soaking experiments. Modifications of the crystallization conditions were needed to get crystals of the complex with nucleotide, as explained under "Experimental Procedures." The crystals grown with GTP diffracted very well, to 2.1 Å resolution. Crystals with GDP grew under similar conditions but only diffracted to 3 Å resolution.

GTP is bound in the ATP-grasp fold of the amino-terminal domain of the β-subunit of pig GTP-specific SCS (Fig. 1). Fig. 1*B* shows the electron density for GTP and a potassium ion. The interactions providing the specific binding of the guanine base are hydrogen-bonding interactions between the side chain of Gln-20β and O-6 of the base and between the amide nitrogen and carbonyl oxygen atoms of Leu-109β and O-6, N-1, and N-2 of the base. The γ-phosphate of GTP interacts with the guanidinium group and amide nitrogen atom of Arg-54β, the amide nitrogen atom of Gly-53β and the side chain of Asp-220β. Although Lys-222β is also within hydrogen-bonding distance of the γ-phosphate, there is no electron density for the amino group of this side chain, indicating that it is disordered and does not interact strongly with the γ-phosphate. Electron density is visible for only one ion bridging the α- and β-phosphates of GTP, as well as interacting with the carbonyl oxygen atom of Asn-206β and the carboxylate oxygen atom of Asp-220β. Initially, this ion was modeled as magnesium, but it was changed to potassium because of the relatively long distances (2.7–3.0 Å) between it and the oxygen atoms in its coordination shell (53) and the relatively low temperature factor of 22 $Å^2$ compared with the average temperature factor of 40 $Å^2$ for the atoms in GTP. During the final cycles of refinement as potassium, the temperature factor for the ion increased to 33 $Å^2$. His-259α is phosphorylated in the structure of the complex with GTP and in the structures where no nucleotide is bound. It is not phosphorylated in the complex with GDP, but there is electron density for a phosphate ion near His-259α. A second molecule of GTP in complex with a single Mg^{2+} ion is bound at a crystal-packing interface in the structure of the GTP complex. Its interactions with the two pro-

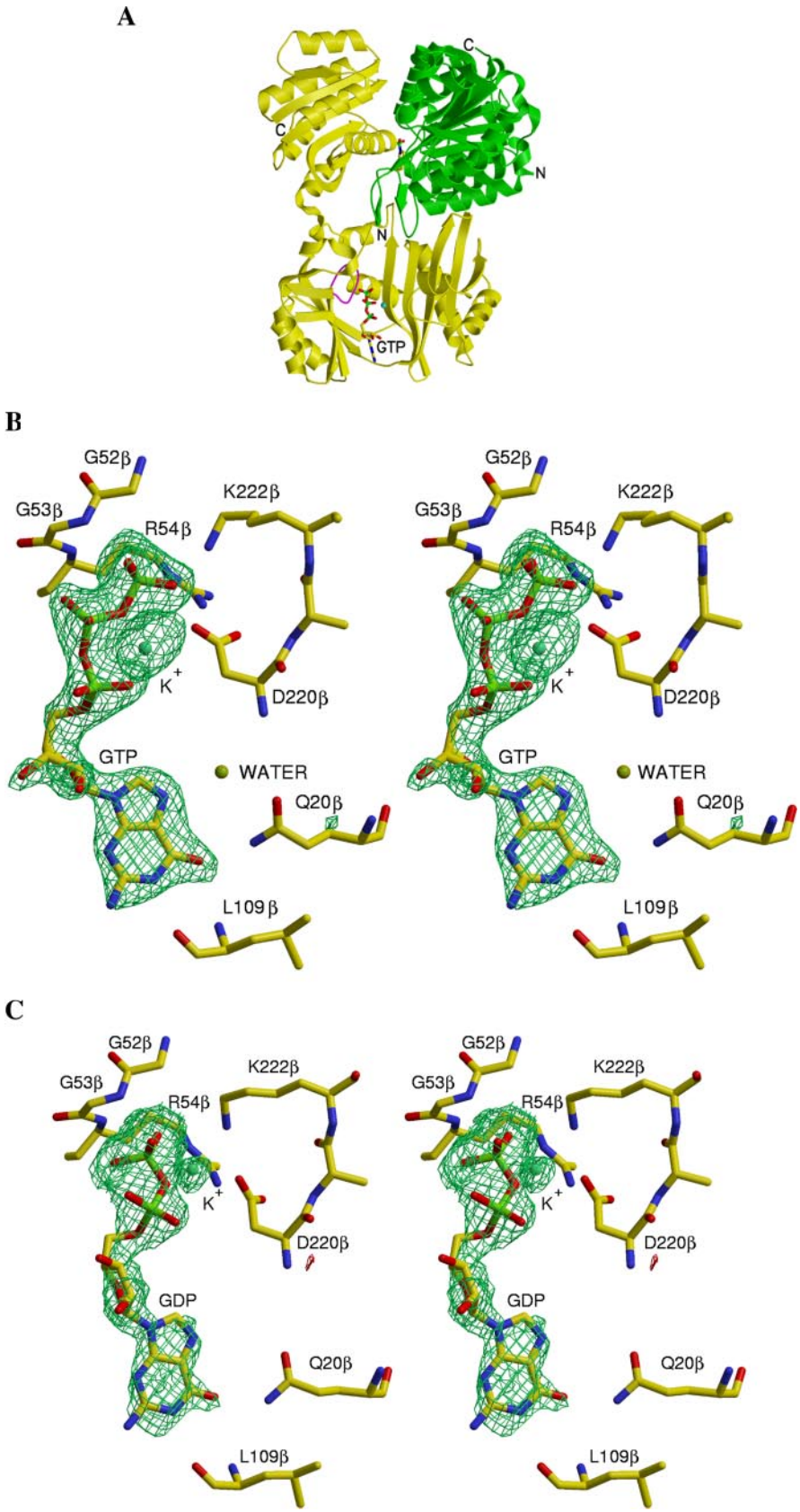

FIGURE 1. *A*, *ribbon diagram* of pig GTP-specific SCS showing the location of the GTP-binding site. The α-subunit is *green*, the β-subunit is *yellow*, except for the T-loop, which is highlighted in *magenta*. GTP, the potassium ion, and the side chain of the phosphorylated histidine residue, His-259α, are drawn as *stick models* and colored according to atom type: *red* for oxygen, *yellow* for carbon, *blue* for nitrogen, *green* for phosphorus, and *turquoise* for potassium. *B*, stereo view of the electron density for GTP and the potassium ion, including nearby residues of the ATP-grasp domain of pig GTP-specific SCS. The $F_o - F_c$, α_c electron density map calculated without GTP and the potassium ion is contoured at 3 σ. *C*, stereo view of the electron density for GDP and the potassium ion, including nearby residues of the ATP-grasp domain of pig GTP-specific SCS. The $F_o - F_c$, α_c electron density map calculated without GDP and the potassium ion is contoured at 3 σ. The same atom colors were used in *B* and *C* as described for *A*. All parts of the figure were drawn using the program RASTER3D (58), and *B* and *C* also used the program XFIT (47).

tein molecules may explain why this crystal diffracts so well compared with the crystals of the complex with GDP. A small amount of electron density is visible in the same crystal-packing site in the complex of GDP with SCS, possibly because of contamination of GDP with GTP or because of phosphorylation of the protein, which could then lead to phosphorylation of GDP during crystallization. There is also extra den-

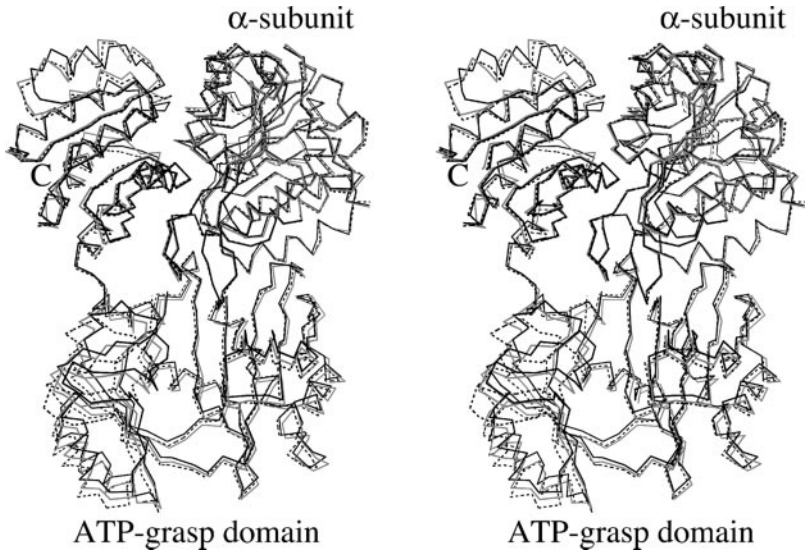

FIGURE 2. **Stereo view of the superposition of the Cα trace of pig GTP-specific SCS bound to GTP (*solid black line*) and the Cα traces of the two nucleotide-free structures determined in this work (*dashed black line*, without chloride and *solid gray line*, with chloride).** The superpositions were based solely on residues of the α-subunit.

sity at the GDP-binding site that could be attributed to some GTP bound at this site. Due to the low resolution of the diffraction data, only GDP was modeled in the nucleotide-binding site. Fig. 1*C* shows the electron density for GDP and the potassium ion.

DISCUSSION

The structures of pig GTP-specific SCS without bound nucleotide demonstrate that the domain possessing the ATP-grasp fold exists in both the open and the closed form in the absence of nucleotide. Analysis of the domain movement based on the first structure solved in this work and the structure of dephosphorylated pig GTP-specific SCS (Protein Data Bank identifier 1EUC) (36) indicates that the smaller domain consists of residues 3–7 and 20–109, while the second "domain" consists of residues 8–19 and 110–390 of the β-subunit. Clearly, the COOH-terminal domain of the β-subunit stays fixed relative to the larger subdomain of the ATP-grasp fold. Interactions of the β-subunit with the α-subunit involve only residues of the larger subdomain of the ATP-grasp fold and the COOH-terminal domain of the β-subunit. Therefore, there does not appear to be any way of communicating the open or closed state of the ATP-grasp fold to the α-subunit, in particular to the phosphohistidine loop. The phosphohistidine loop is seen in all structures bound to the rest of the α-subunit, independent of whether the domain possessing the ATP-grasp fold is open or closed.

The nucleotide binds in the domain possessing the ATP-grasp fold as predicted, but surprisingly the γ-phosphate is tightly bound to the protein and not free to react as is the γ-phosphate of nucleoside triphosphates bound to other proteins possessing the ATP-grasp fold. When either GTP or GDP is bound to SCS, the binding domain is in the closed conformation. Comparisons can be made with the two nucleotide-free structures determined in this work, one of which included chloride ions in the crystallization solution (Fig. 2). The different conformations support the view that this domain is flexible, since it has been trapped by the crystallization experiment with different degrees of opening. A difference between SCS and other ATP-grasp proteins is that the phosphate-binding loop, nicknamed the T-loop, is disordered in glycinamide ribonucleotide transformylase unless ATP is bound (54). In the structures of SCS, the equivalent loop (highlighted in Fig. 1*A*), which includes Arg-54β, is ordered and adopts a similar conformation whether it is bound to ADP (7), GTP and GDP (this paper), or no nucleotide (4, 5, 36). The phosphate-binding loop in SCS is preformed, just like the P-loops of other ATP-binding proteins. In contrast to the T-loop of glycinamide ribonucleotide transformylase, which in conjunction with a loop from the side of the ATP-grasp domain shields the phosphate groups of ATP from the solvent, the T-loop of SCS interacts from the side, with Arg-54β buried beneath GTP or GDP. The T-loop of SCS can be preformed because there is no need for it to change conformation to allow nucleotide to bind.

A comparison of the structure of GTP bound to pig GTP-specific SCS with the structure of ADP bound to *E. coli* SCS (7) indicates which interactions lead to specificity for the guanine base. In contrast to the GTP-specific enzyme, *E. coli* SCS can use both ATP and GTP, although ATP is preferred. The interactions with the guanine base in the complex of GTP with GTP-specific SCS are provided by the glutamine residue, Gln-20β, and the backbone atoms of Leu-109β, as shown in Fig. 3*A*. The glutamine side chain interacts directly with the guanine base through a hydrogen bond donated to O-6 and it interacts indirectly through a water molecule that forms a hydrogen bond with N-7. Fig. 3*A* shows that the adenine base of ADP bound to *E. coli* SCS is located further into the binding pocket relative to GTP bound to pig GTP-specific SCS. The side chain of the proline residue of *E. coli* SCS at the position equivalent to Gln-20β of GTP-specific SCS is considerably shorter, allowing for the different position of the base. When the two complexes are superposed, N-1 of the adenine base is in a similar position to O-6 of the guanine base and forms a comparable hydrogen bond with the backbone amide nitrogen atom. In the complex of ADP with *E. coli* SCS, N-6 of the adenine base interacts with the carbonyl oxygen atom of Ala-100β and with the side chain of Glu-99β. When GTP or GDP binds to the *E. coli* SCS, it is likely that a water molecule would be trapped between the side chain of the proline residue and the base, near the position of N-6 of ADP, providing interactions with the guanine base, Ala-100β and Glu-99β. The presence of Pro-20β in *E. coli* SCS allows this enzyme to bind either ATP or GTP, whereas Gln-20β leads to the nucleotide specificity of GTP-specific SCS. This analysis can be extended to the forms of SCS from human, mouse, pigeon, and *Caenorhabditis elegans*, which are proposed to be GTP-specific, since all have a glutamine residue in the equivalent position to that of pig (1). However, the ATP-specific forms from the same species have proline at this position just like *E. coli* SCS, so it is not clear what leads to their nucleotide specificity.

The γ-phosphate of GTP is tightly bound to pig GTP-specific SCS and the conformation of GTP would have to change for the γ-phosphate to become available for transfer to the active site histidine residue. Based on mutagenesis experiments using *E. coli* SCS (55), during the

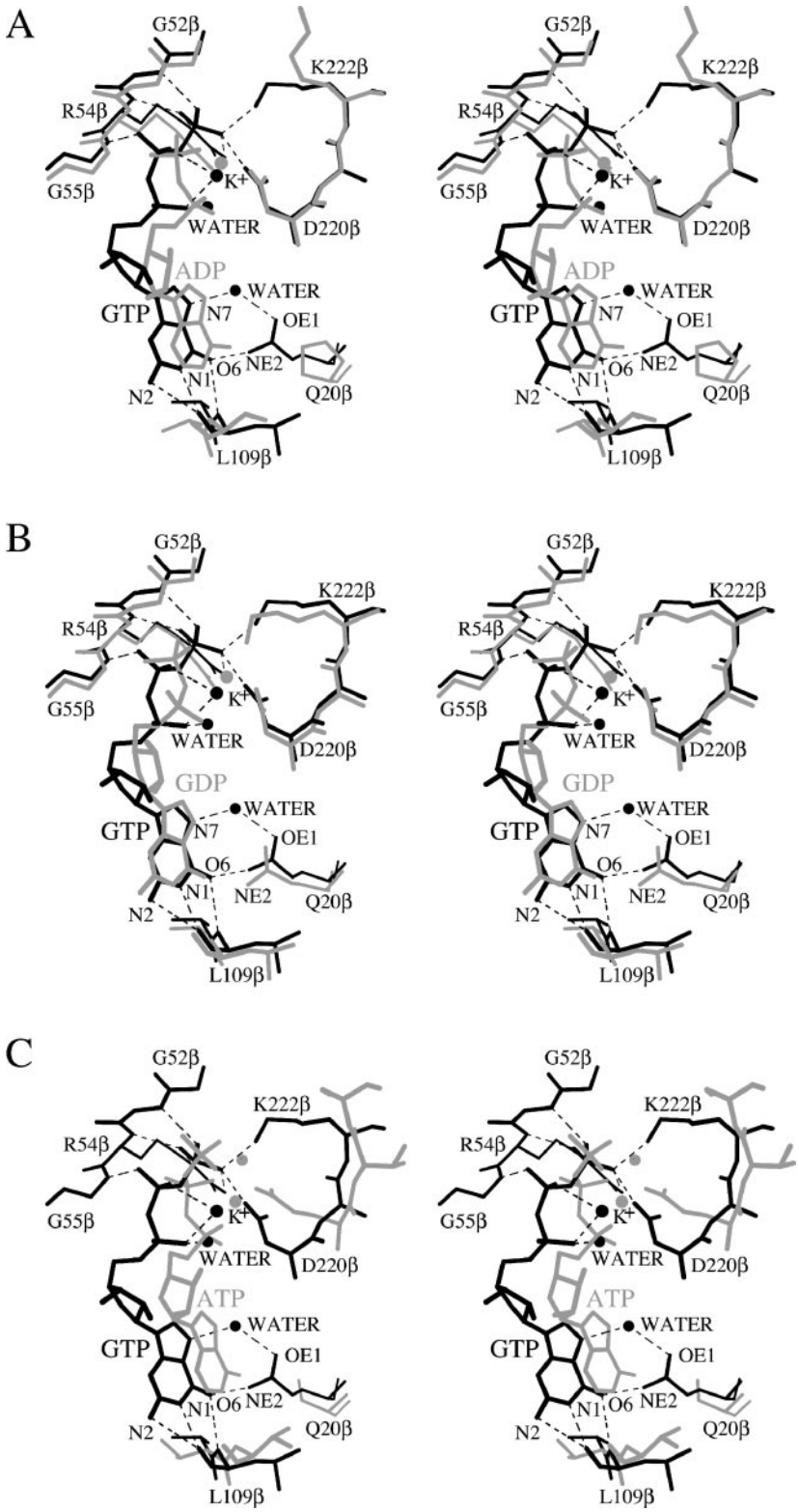

FIGURE 3. **Stereo views of the superpositions of GTP bound to pig GTP-specific SCS (*black*) with ADP bound to *E. coli* SCS (*gray*) (Protein Data Bank (43) identifier 1cqi (7)) (*A*), GDP bound to pig GTP-specific SCS (*gray*) (*B*), and ATP bound to glycinamide ribonucleotide transformylase (*gray*) (PDB identifier 1kj8) (54) (*C*).** The superpositions were based on structurally similar residues and performed using the program O (51) with a cutoff of 3.8 Å. Possible hydrogen-bonding interactions and ionic interactions between GTP and the pig GTP-specific SCS are represented by *black dashed lines*.

phosphorylation by GTP, His-259α would bind near Glu-204β, interacting via a hydrogen bond just as the equivalent glutamate residue of *E. coli* SCS does. For an understanding of what changes in the conformation of GTP must take place for the γ-phosphate to become available, two structural comparisons are useful. The first is the structural comparison of the complex of GTP and SCS with the complex of GDP and SCS. The second is the structural comparison of the complex of GTP and SCS with the complex of ATP and other ATP-grasp proteins. Fig. 3*B* is a close-up view of the nucleotide-binding site showing the superposition of the complex of SCS with GTP and its complex with GDP. Only a small change in the orientation of the guanine base would be needed, but the ribose moiety and the α-phosphate must move further into the binding pocket for GTP to bind like GDP does. In both the complex with GTP and the complex with GDP, the ion bridges the α-

and β-phosphate groups. The same is true in the complex of ADP with glycinamide ribonucleotide transformylase (data not shown) (54). However, in the complex of ATP with glycinamide ribonucleotide transformylase, the similarly positioned ion bridges the α- and γ-phosphate groups. Fig. 3*C* shows the superposition of the complex of ATP with glycinamide ribonucleotide transformylase and the complex of GTP with SCS (54). All of the interactions of the oxygen atoms of the triphosphate of GTP would have to break and be reformed for GTP to adopt the same conformation as seen for ATP in glycinamide ribonucleotide transformylase. The second ion in the complex of ATP with glycinamide ribonucleotide transformylase bridges the β- and γ-phosphates. The positively charged side chain of Lys-222β of pig GTP-specific SCS might serve the role of this ion, but since this lysine residue is not strictly conserved in SCS, there is likely to be a second metal ion needed for binding the nucleotide in the conformation that allows the transfer of the phosphoryl group. The oxygen atom of the γ-phosphate lying near the second metal ion-binding site in the superposition shown in Fig. 3*C* may be protonated, since the distance between it and Asp-220β suggest that they are hydrogen-bonded to each other. It is more likely that the γ-phosphate is protonated than Asp-220β because Asp-220β interacts with the positively charged potassium ion. The γ-phosphate interacts with Arg-54β and Lys-222β, but the interaction with Lys-222β is weak, as explained under "Results," and this may be due to protonation of the γ-phosphate. The charge on GTP would be different if the two magnesium ions were present and if the γ-phosphate were in position to phosphorylate the active site histidine residue.

The most interesting discovery in this work is that phosphorylated SCS is able to bind nucleotide triphosphate in such a way that the nucleotide is protected from hydrolysis. Originally, it was thought that phosphorylated *E. coli* SCS could not even bind ATP (56). Later, it was shown that the H142αN mutant of *E. coli* SCS not only bound ATP but catalyzed the phosphorylation of ATP to produce adenosine 5′-tetraphosphate (57). This result was interpreted to suggest that the mutation caused a conformational change, allowing ATP to bind even when the active site histidine residue was phosphorylated. The structure of the complex of GTP with phosphorylated SCS proves that nucleotide triphosphate can bind to phosphorylated enzyme. His-142α of *E. coli* SCS and the equivalent residue of pig GTP-specific SCS, His-151α, are each located ~15 Å from the active site histidine residue. The γ-phosphate group of GTP is located 45 Å from His-151α and 32 Å from the phosphohistidine. There would be a greater likelihood of the mutation affecting binding of the active-site histidine residue than affecting the binding of nucleotide triphosphate based on these distances. It may be that the mutation destabilizes the conformation of the phosphohistidine loop that has been seen in the structures, leading it to lose its noncovalent interactions with the α-subunit and flip into position to phosphorylate the nucleotide. Based on the structure of the complex of GTP with pig GTP-specific SCS, the γ-phosphate would be protected from hydrolysis, but since it is in the same position as the β-phosphate of GDP, it would be in position to be phosphorylated. One way to test this hypothesis is by mutating His-151α, testing whether the mutant catalyzes the formation of guanosine tetraphosphate and, if it does, determining the structure of the complex with GTP or guanosine tetraphosphate.

The major question left from this analysis is how the reaction phosphorylating the active site histidine residue would take place. In this case, the phosphohistidine loop must flip into position for the histidine residue to be phosphorylated. The conformation of GTP would then have to change, likely to a position similar to that seen for ATP bound to other members of the family of proteins with ATP-grasp folds, to make the γ-phosphate available for phosphorylation of the histidine residue.

Acknowledgments—We thank William T. Wolodko for critically reading and commenting on the manuscript. X-ray diffraction data for the complexes of pig GTP-specific SCS with GTP and with GDP were collected at beamline 8.3.1 of the Advanced Light Source (ALS) at Lawrence Berkeley Laboratory, under an agreement with the Alberta Synchrotron Institute (ASI). The ALS is operated by the Department of Energy and supported by the National Institute of Health. Beamline 8.3.1 was funded by the National Science Foundation, the University of California, and Henry Wheeler. The ASI synchrotron access program is supported by grants from the Alberta Science and Research Authority and the Alberta Heritage Foundation for Medical Research. X-ray diffraction data for nucleotide- and chloride-free pig GTP-spcific SCS were collected at beamline 14-BM-C of the Advanced Photon Source (APS). Use of the APS was supported by the United States Department of Energy, Basic Energy Sciences, Office of Science, under Contract No. W-31-109-Eng-38. Use of the BioCARS Sector 14 was supported by the National Institutes of Health, National Center for Research Resources, under Grant RR07707.

REFERENCES

1. Johnson, J. D., Mehus, J. G., Tews, K., Milabetz, B. I., and Lambeth, D. O. (1998) *J. Biol. Chem.* **273,** 27580–27586
2. Johnson, J. D., Muhonen, W. W., and Lambeth, D. O. (1998) *J. Biol. Chem.* **273,** 27573–27579
3. Murzin, A. G. (1996) *Curr. Opin. Struct. Biol.* **6,** 386–394
4. Wolodko, W. T., Fraser, M. E., James, M. N. G., and Bridger, W. A. (1994) *J. Biol. Chem.* **269,** 10883–10890
5. Fraser, M. E., James, M. N. G., Bridger, W. A., and Wolodko, W. T. (1999) *J. Mol. Biol.* **285,** 1633–1653
6. Joyce, M. A., Fraser, M. E., Brownie, E. R., James, M. N. G., Bridger, W. A., and Wolodko, W. T. (1999) *Biochemistry* **38,** 7273–7283
7. Joyce, M. A., Fraser, M. E., James, M. N. G., Bridger, W. A., and Wolodko, W. T. (2000) *Biochemistry* **39,** 17–25
8. Murzin, A. G., Brenner, S. E., Hubbard, T., and Chothia, C. (1995) *J. Mol. Biol.* **247,** 536–540
9. Yamaguchi, H., Kato, H., Hata, Y., Nishioka, T., Kimura, A., Oda, J., and Katsube, Y. (1993) *J. Mol. Biol.* **229,** 1083–1100
10. Polekhina, G., Board, P. G., Gali, R. R., Rossjohn, J., and Parker, M. W. (1999) *EMBO J.* **18,** 3204–3213
11. Fan, C., Moews, P. C., Walsh, C. T., and Knox, J. R. (1994) *Science* **266,** 439–443
12. Roper, D. I., Huyton, T., Vagin, A., and Dodson, G. (2000) *Proc. Natl. Acad. Sci. U. S. A.* **97,** 8921–8925
13. Kuzin, A. P., Sun, T., Jorczak-Baillass, J., Healy, V. L., Walsh, C. T., and Knox, J. R. (2000) *Struct. Fold. Des.* **8,** 463–470
14. Sakai, H., Vassylyeva, M. N., Matsuura, T., Sekine, S., Gotoh, K., Nishiyama, M., Terada, T., Shirouzu, M., Kuramitsu, S., Vassylyev, D. G., and Yokoyama, S. (2003) *J. Mol. Biol.* **332,** 729–740
15. Waldrop, G. L., Rayment, I., and Holden, H. M. (1994) *Biochemistry* **33,** 10249–10256
16. Wang, W., Kappock, T. J., Stubbe, J., and Ealick, S. E. (1998) *Biochemistry* **37,** 15647–15662
17. Thoden, J. B., Kappock, T. J., Stubbe, J., and Holden, H. M. (1999) *Biochemistry* **38,** 15480–15489
18. Thoden, J. B., Firestine, S., Nixon, A., Benkovic, S. J., and Holden, H. M. (2000) *Bicohemistry* **39,** 8791–8802
19. Thoden, J. B., Holden, H. M., Wesenberg, G., Raushel, F. M., and Rayment, I. (1997) *Biochemistry* **36,** 6305–6316
20. Esser, L., Wang, C., Hosaka, M., Smagula, C. S., Sudhof, T. C., and Deisenhofer, J. (1998) *EMBO J.* **17,** 977–984
21. Herzberg, O., Chen, C. C. H., Kapadia, G., McGuire, M., Carroll, L., Noh, S. J., and Dunaway-Mariano, D. (1996) *Proc. Natl. Acad. Sci. U. S. A.* **93,** 2652–2657
22. Subramanya, H. S., Doherty, A. J., Ashford, S. R., and Wigley, D. B. (1996) *Cell* **85,** 607–615
23. Singleton, M. R., Hakansson, K., Timson, D. J., and Wigley, D. B. (1999) *Struct. Fold. Des.* **7,** 35–42
24. Hakansson, K., Doherty, A. J., Shuman, S., and Wigley, D. B. (1997) *Cell* **89,** 545–553
25. Ho, C. K., Wang, L. K., Lima, C. D., and Shuman, S. (2004) *Structure (Camb.)* **12,** 327–339
26. Kaufman, S., Gilvarg, C., Cori, O., and Ochoa, S. (1953) *J. Biol. Chem.* **203,** 869–888
27. Murakami, K., Mitchell, T., and Nishimura, J. S. (1972) *J. Biol. Chem.* **247,** 6247–6254
28. Kaufman, S., and Alivisatos, S. G. A. (1955) *J. Biol. Chem.* **216,** 141–152

29. Hamilton, M. L., and Ottaway, J. H. (1981) *FEBS Lett.* **123,** 252–254
30. Ottaway, J. H., McClellan, J. A., and Saunderson, C. L. (1981) *Int. J. Biochem.* **13,** 401–410
31. Smith, C. M., Bryla, J., and Williamson, J. R. (1974) *J. Biol. Chem.* **249,** 1497–1505
32. McClellan, J. A., and Ottaway, J. H. (1980) *Comp. Biochem. Physiol. B* **67,** 679–684
33. Labbe, R. F., Kurumada, T., and Onisawa, J. (1965) *Biochim. Biophys. Acta* **111,** 403–415
34. Lambeth, D. O., Tews, K. N., Adkins, S., Frohlich, D., and Milavetz, B. I. (2004) *J. Biol. Chem.* **279,** 36621–36624
35. Elpeleg, O., Miller, C., Hershkovitz, E., Bitner-Glindzicz, M., Bondi-Rubinstein, G., Rahman, S., Pagnamenta, A., Eshhar, S., and Saada, A. (2005) *Am. J. Hum. Genet.* **76,** 1081–1086
36. Fraser, M. E., James, M. N. G., Bridger, W. A., and Wolodko, W. T. (2000) *J. Mol. Biol.* **299,** 1325–1339
37. Bailey, D. L., Wolodko, W. T., and Bridger, W. A. (1993) *Protein Sci.* **2,** 1255–1262
38. Murakami, Y., and Nishimura, J. S. (1974) *Biochim. Biophys. Acta* **336,** 252–263
39. Cha, S. (1969) *Methods Enzymol.* **13,** 62–69
40. Otwinowski, Z., and Minor, W. (1997) *Methods Enzymol.* **276,** 307–326
41. Holton, J., and Alber, T. (2004) *Proc. Natl. Acad. Sci. U. S. A.* **101,** 1537–1542
42. Collaborative Computational Project, No. 4 (1994) *Acta Crystallogr. Sect. D Biol. Crystallogr.* **50**, 760–763
43. Berman, H. M., Westbrook, J., Feng Z., Gilliland, G., Bhat, T. N., Weissig, H., Shindyalov, I. N., and Bourne, P. E. (2000) *Nucleic Acids Res.* **28,** 235–242
44. Navaza, J. (1994) *Acta Crystallogr. Sect. A* **50**, 157–163
45. Brunger, A. T., Adams, P. D., Clore, G. M., Delano, W. L., Gros, P., Grosse-Kunstleve, R. W., Jiang, J.-S., Kuszewski, J., Jilges, N., Pannu, N. S., Read, R. J., Rice, L. M., Simonson, T., and Warren, G. L. (1998) *Acta Crystallogr. Sect. D Biol. Crystallogr.* **54**, 905–921
46. Jones, T. A. (1985) *Methods Enzymol.* **115,** 157–171
47. McRee, D. E. (1999) *J. Struct. Biol.* **125,** 156–165
48. Laskowski, R. A., MacArthur, M. W., Moss, D. S., and Thornton, J. M. (1993) *J. Appl. Crystallgor.* **26,** 283–291
49. Hooft, R. W. W., Vriend, G., Sander, C., and Abola, E. E. (1996) *Nature* **381,** 272
50. Guex, N., and Peitsch, M. C. (1997) *Electrophoresis* **18,** 2714–2723
51. Jones, T. A., Zou, J. Y., Cowan, S. W., and Kjeldgaard, M. (1991) *Acta Crystallogr. Sect. A* **47**, 110–119
52. Hayward, S., and Berendsen, H. J. C. (1998) *Proteins Struct. Funct. Genet.* **30,** 144–154
53. Harding, M. M. (2002) *Acta Crystallogr. Sect. D Biol. Crystallogr.* **58**, 872–874
54. Thoden, J. B., Firestine, S. M., Benkovic, S. J., and Holden, H. M. (2002) *J. Biol. Chem.* **277,** 23898–23908
55. Fraser, M. E., Joyce, M. A., Ryan, D. G., and Wolodko, W. T. (2002) *Biochemistry* **41,** 537–546
56. Bowman, C. M., and Nishimura, J. S. (1975) *J. Biol. Chem.* **250,** 5609–5613
57. Luo, G.-X., and Nishimura, J. S. (1992) *J. Biol. Chem.* **267,** 9516–9520
58. Merritt, E. A., and Bacon, D. J. (1997) *Methods Enzymol.* **277,** 505–524